Laboratory Investigation (2021) 101:865–877
https://doi.org/10.1038/s41374-021-00575-9

ARTICLE

6-Gingerol relieves myocardial ischaemia/reperfusion injury by regulating lncRNA H19/miR-143/ATG7 signaling axis-mediated autophagy

Xiang-Wei Lv[1] · Meng-Jie Wang[2] · Qiu-Yu Qin[1] · Pan Lu[1] · Guo-Wei Qin[3]

Received: 24 September 2020 / Revised: 21 January 2021 / Accepted: 21 January 2021 / Published online: 23 March 2021

Abstract

Myocardial ischemia/reperfusion injury (MIRI) causes severe damage in cardiac tissue, thereby resulting in a high rate of mortality. 6-Gingerol (6-G) is reported to play an essential role in alleviating MIRI. However, the underlying mechanism remains obscure. This study was intended to explore the potential mechanism by which 6-G functions. Q-PCR was employed to quantify the relative RNA levels of long noncoding RNA (lncRNA) H19 (H19), miR-143, and ATG7, an enzyme essential for autophagy, in HL-1 cells. Western blotting, immunofluorescence, and immunohistochemistry were employed for protein evaluation in cultured cells or mouse tissues. Cell viability, cytotoxicity, and apoptosis were analysed by CCK-8, LDH, and flow cytometry assays, respectively. The binding sites for miR-143 were predicted using starBase software and experimentally validated through a dual-luciferase reporter system. Here, we found that 6-G elevated cellular H19 expression in hypoxia/reoxygenation (H/R)-treated HL-1 cells. Moreover, 6-G increased Bcl-2 expression but reduced cleaved caspase 3 and caspase 9 protein levels. Mechanistically, H19 directly interacted with miR-143 and lowered its cellular abundance by acting as a molecular sponge. Importantly, ATG7 was validated as a regulated gene of miR-143, and the depletion of miR-143 by H19 caused an increased in ATG7 expression, which in turn promoted the autophagy process. Last, mouse experiments highly supported our in vitro findings that 6-G relieves MIRI by enhancing autophagy. The H19/miR-143/ATG7 axis was shown to be critical for the function of 6-G in relieving MIRI.

Introduction

Acute myocardial infarction (AMI) is a leading threat to human health and survival worldwide and confers high morbidity and mortality [1]. Currently, rapid reperfusion is a dominant strategy for the treatment of AMI, which, however, induces abnormal cardiac functions, such as myocardial ischemia/reperfusion injury (MIRI) [2]. Clinically, thrombolytic therapy or percutaneous coronary intervention is a widely adopted therapeutic strategy to reduce the incidence of subsequent heart failure and mortality [3]. The mortality rate of MIRI is still as high as 10% among AMI patients who receive rapid reperfusion therapy [4]. Thus, there is an urgent demand to develop novel drugs to prevent mortality caused by MIRI.

Thus far, knowledge about the cellular mechanisms underlying MIRI is still extremely limited. Previous findings indicated that cellular oxidative induction, inflammatory responses, $Ca2^{+}$ overload, and apoptosis contribute substantially to the incidence and pathophysiology of MIRI [5].

These authors jointly supervised this work: Xiang-Wei Lv, Meng-Jie Wang

Supplementary information The online version contains supplementary material available at https://doi.org/10.1038/s41374-021-00575-9.

✉ Guo-Wei Qin
qinguowei@glmc.edu.cn

[1] Department of Cardiology, Affiliated Hospital of Guilin Medical University, Guilin, Guangxi Zhuang Autonomous Region, P.R. China

[2] Department of Cardiology, The People's Hospital of Guangxi Zhuang Autonomous Region, Nanning, Guangxi Zhuang Autonomous Region, P.R. China

[3] Department of Science and Technology, Guilin Medical University, Guilin, Guangxi Zhuang Autonomous Region, P.R. China

Among these, an increasing number of reports have documented that inhibiting the apoptosis of cardiomyocytes contributes greatly to alleviating MIRI [6, 7]. Autophagy is an important intracellular degradation process that can be triggered by cellular stress, such as hypoxia, energy depletion, nutrient deprivation, and ER stress [8]. Previously, autophagy was believed to play a protective role in alleviating MIRI [9]. Our pilot research showed that autophagy is closely involved in the pathophysiology of MIRI, which suggested a significantly reduced autophagy level in the MIRI model. Accordingly, exploring core factors involved in MIRI and developing a rational intervention to reduce apoptosis or promote autophagy following ischemia-reperfusion is of great clinical significance.

Noncoding RNAs, including long noncoding RNAs (lncRNAs, > 200 nt) and microRNAs (miRNAs, approximately 20–22 nt), have already been extensively studied in the last decade. Accumulating reports have indicated a close association of lncRNAs with MIRI [10, 11]. Among these lncRNAs, lncRNA H19, a core regulator in embryonic development [12, 13], has also been widely indicated to be involved in MIRI by regulating miRNA-dependent pathways [14, 15]. Interestingly, Zhou et al. reported that H19 could protect mice from AMI by activating autophagy [16]. These results greatly prompted us to explore potential drugs targeting the H19 regulatory axis, which may provide a novel therapeutic strategy for AMI.

Encouragingly, ginger, an ancient traditional medicinal and edible plant, has broad applications in treating cardiovascular diseases for thousands of years in China. 6-Gingerol (6-G), a core ingredient in ginger, plays critical roles in regulating inflammation as well as the PI3K/Akt signaling pathway [17, 18]. However, it is still unclear whether 6-G is involved in regulating H19-mediated MIRI alleviation.

Therefore, we performed the present study to investigate whether and how 6-G regulates H19-mediated MIRI alleviation. We revealed that cellular H19 was upregulated by 6-G and subsequently promoted the autophagy process, which in turn provided myocardial protection against MIRI.

Materials and methods

Cell culture and treatment

HL-1 cells were commercially provided by American Type Culture Collection (ATCC, VA, USA) and maintained in Claycomb Medium supplemented with 10% FBS, 100 μM norepinephrine, 2 mM L-glutamine, 100 U/ml streptomycin, and 100 U/ml penicillin at 37 °C with 5% CO_2. For hypoxia/reoxygenation (H/R) treatment, 10^5 cells were prepared in 6-well plates and incubated in a hypoxia chamber (94% N_2, 5% CO_2 and 1% O_2 at 37 °C) for 16 h. Thereafter, the cells were incubated in an atmosphere of 5% CO_2 for 6 h. To evaluate the effect of 6-G on H/R-induced MIRI, different experimental groups were established as follows: (1) control group (cultured under normal culture conditions); (2) H/R-challenged group; (3) H/R-treated cells cultured with 20 μM 6-G; and (4) other components added accordingly, such as 3-methyladenine (3-MA; 5 mM), chloroquine (CQ; 10 μM), sh NC (60 nM), sh H19 (60 nM), miR-143 inhibitor (60 nM), and pcDNA3.1-ATG7 (1 μg). The cells were then harvested for subsequent assays.

Plasmid construction and cell transfection

The shRNA oligonucleotides against H19 were synthesized by GenePharma (Shanghai, China) and cloned into the pLKO.1 puro vector (Addgene, USA). ATG7 cDNA was acquired through RT-PCR and then cloned into the pcDNA 3.1-expressing vector (Invitrogen). The transfection of the indicated constructs was conducted by using Lipofectamine 3000 following the manufacturer's guidance (Invitrogen, USA). After 48 h, the cells were used for subsequent experiments.

Cell viability assay

Cell viability was determined by a CCK-8 kit (Donjindo) according to the manufacturer's instructions. Briefly, 1×10^3 cells were plated in 96-well plates and incubated overnight. Then, cells in each well were mixed with 10 μl CCK-8 solution and incubated for 2 h. The absorbance at 450 nm was measured using a microplate reader (Bio-Rad, Hercules, CA, USA).

Cytotoxicity assay

The cytotoxic activity was determined by measuring the level of lactate dehydrogenase (LDH) in the medium with an LDH Cytotoxicity Detection Kit (Roche, Basel, Switzerland) according to the manufacturer's instructions. The absorbance of each well was determined at 490 nm using a microplate reader (Becton Dickinson, USA).

Cell apoptosis assay

HL-1 cells were pretreated with 6-G and transfected with the indicated plasmids. Twenty-four hours later, cells from each well were collected and washed with PBS. The cells were then incubated with 5 μl of annexin V-fluorescein isothiocyanate for 15 min, followed by 2 μl of propidium iodide (PI) for 10 min. Apoptotic cells were quantified by a flow cytometer (BD Biosciences, USA).

Table 1 Primer sequences for quantitative PCR.

Gene	Forward sequence	Reverse sequence
H19	5′-AAGAGCTCGGACTGGAGACT-3′	5′-AAGAAGGCTGGATGACTGCC-3′
miR-143-3p	5′-GAGATGAAGCACTGTAGCT-3′	5′-GCACAGAATCA ACACGACTCACTAT-3′
ATG7	5′-CCTGTGAGCTTGGATCAAAGGC-3′	5′-GAGCAAGGAGACCAGAACAGTG-3′
U6	5′-CTCGCTTCGGCAGCACA-3′	5′-AACGCTTCACGAATTTGCGT-3′
GAPDH	5′-AGCCCAAGATGCCCTTCAGT-3′	5′-CCGTGTTCCTACCCCCAATG-3′

RNA extraction and quantitative PCR

Total RNA extraction was completed by using TRIzol reagent (Invitrogen, USA). Total RNA was reverse transcribed into cDNA using a cDNA synthesis kit (Thermo Fisher). Gene expression was quantitatively analysed by using SYBR green with the 7500 Real-Time PCR system (Takara, China). The $2^{-\Delta\Delta Ct}$ method was applied to calculate the relative expression of genes using GAPDH and U6 RNA as reference genes. The PCR primers for the qPCR are listed in Table 1.

Immunofluorescence

HL-1 cells were collected and seeded on cover slips. Next, cells were fixed with methanol for 30 min at −20 °C. After washing with PBS, cells were blocked with 5% BSA for 2 h, followed by incubation with LC3 antibody (1:2000, ab51520, Abcam) overnight at 4 °C. The next day, cells were incubated with Alexa Fluor 546-conjugated secondary antibody (1:200, Invitrogen, USA) for 2 h and stained with DAPI to visualize DNA. The images were acquired using fluorescence microscopy.

Autophagic flux assay

HL-1 cells were cultured and transfected with mRFP-GFP-LC3B adenovirus according to the manufacturer's instructions (Hanbio, China). After 24 h of transfection, cells were washed with PBS and then treated as indicated groups. After 48 h of treatment, the cells were washed with PBS, fixed with 4% paraformaldehyde, and stained with DAPI. The fluorescence was observed under a confocal laser scanning microscope (Zeiss, Germany). Finally, the number of puncta per cell was determined using NIH ImageJ software.

Western blot analysis

HL-1 cells and myocardial tissues were washed and lysed with RIPA lysis buffer (Beyotime, Shanghai, China), and myocardial tissue protein was prepared as previously described [17]. Proteins in lysates were quantified, and 20 μg of total protein was loaded and separated by 10% SDS-PAGE and transferred to a PVDF membrane. The membrane was then blocked in 5% BSA and incubated with primary antibodies: LC-3I (ab239849, 1:500), LC-3II (ab48394, 1:500), Bcl-2 (ab196495, 1:1000), cleaved caspase 3 (ab49822, 1:500), cleaved caspase 9 (ab52298, 1:1000), Beclin-1 (ab210498, 1:1000), p62 (ab56416, 1:1000), ATG7 (ab52472, 1:5000), and β-actin (ab8227, 1:1000). After washing with PBST, the membrane was probed with HRP-labeled goat anti-mouse/rabbit IgG (1:5000, Sigma, USA) for 2 h at room temperature. Finally, signals were visualized using enhanced chemiluminescence reagent (EMD Millipore, USA) and analysed using Image-Pro Plus 6.0 software.

Dual luciferase assays

The wild-type and mutant miR-143 target segments of H19 and ATG7 mRNA 3′-UTRs were inserted into the pGL3 vector (Promega, Madison, USA) and named H19-WT, H19-MUT, ATG7-WT, and ATG7-MUT, respectively. For luciferase reporter assays, HL-1 cells were cotransfected with H19-WT or H19-MUT and miR-143 mimics or NC mimics using Lipofectamine 3000 (Invitrogen). Luciferase activity was measured using the Dual-Luciferase Reporter Assay System (Promega). The examination of the interplay between miR-143 and ATG7 was performed as the same as the validation between miR-143 and H19.

Animals and ethics

Male C57BL/6 mice (25–30 g, 10–12 weeks old) were provided by the Guilin Medical University Animal Experiment Center, reared under standard conditions and had free access to clean drinking water and feed throughout the day. The animal ethics involved in the experiment were approved by the Guilin Medical University Laboratory Animal Ethics Committee. In the animal experiment, all trauma operations were performed under anesthesia (pentobarbital sodium, 40 mg/kg) to avoid bearing pain and suffering.

Animal model and experimental design

Mice were randomly divided into four experimental groups: (1) Sham group: mouse accepted thoracotomy without ligating left anterior descending (LAD) coronary arteries; (2) I/R group: mouse accepted thoracotomy, and their LADs were ligated for 30 min followed by reperfusion for 2 h; (3) 6-G + I/R group: mouse were intravenously injected with 6-G (6 mg/kg) 30 min before LAD ligation and then reperfused for 2 h; (4) 3-MA + 6-G + I/R group: 30 min before LAD ligation, mice were injected with 3-MA (10 mg/kg) and 6-G, and then reperfused for 2 h. The mice were handled as described in our previous study [18].

2,3,5-Triphenyl tetrazolium chloride (TTC) staining

The infarct size of the heart was determined by 1% TTC staining using a protocol published previously with slight modifications [17]. In brief, the heart was rapidly excised and sliced into 2 mm thick coronal slices. After washing with 0.9% saline, the slices were stained with TTC solution. The percentage of infarcted myocardium was calculated using Image-Pro Plus 6.0 software.

Immunohistochemistry and TUNEL assay

The mouse hearts were removed, fixed with 4% paraformaldehyde, and embedded in paraffin for coronal sections, which were then used for immunohistochemical (IHC) staining and TUNEL assays. For IHC staining, sections were incubated with LC3 antibody (1:2000, ab51520, Abcam) overnight at 4 °C, followed by incubation with biotin-labeled secondary antibody. The signals were visualized by using HRP-streptavidin with 3,3′-diaminobenzidine (DAB) substrate. The number of apoptotic cells in cardiac slices was evaluated by a TUNEL assay kit (#11684817910, Roche, Germany) according to the manufacturer's instructions. Heart sections were observed under a light microscope (Leica, Germany), and the images were analysed using Image-Pro Plus 6.0 software.

Statistical analysis

The groups were compared using Student's *t*-tests or one-way ANOVA in GraphPad Prism (version 5.01; California, USA). The data were collected from triplicates, are representative of at least three independent experiments and are presented as the means ± SD; *P* values less than 0.05 were considered statistically significant.

Results

6-G attenuates H/R-induced cardiomyocyte injury and enhances autophagy

First, we established an MIRI model in vitro by inducing HL-1 cells under H/R conditions and further investigated the potential role of 6-G in MIRI. As expected, we found that H/R induced decreases in cell viability compared with that of the control, which was partially reversed by treatment with 6-G (Fig. 1A). Additionally, H/R caused increased cell membrane damage and apoptosis. However, it is interesting to observe that 6-G clearly reduced cell apoptosis and cytotoxicity triggered by H/R (Fig. 1B, C). Moreover, H/R injury significantly increased the protein level of cellular proapoptotic factors such as caspase 3 and caspase 9 but decreased the expression of the antiapoptotic gene Bcl-2 (Fig. 1D). Autophagy has been extensively reported to be associated with hypoxia, which motivated us to evaluate the effect of 6-G on autophagic flux. As shown in Fig. 1E, we assessed the autophagic flux in cells transfected with tandem fluorescent mRFP-GFP-LC3B. The results indicated that H/R treatment largely reduced yellow and red puncta, while additional treatment with 6-G clearly restored the number of yellow and red puncta. Moreover, LC3 expression was significantly decreased in H/R-treated cells compared with that in control cells as determined by western blot (Fig. 1F). Notably, the addition of 6-G could clearly restore the LC3II level suppressed by H/R treatment. LncRNA H19 was believed to be a contributor to relieving MIRI. Here, we demonstrated decreased expression of H19 in H/R-treated cells, which was rescued in the presence of 6-G (Fig. 1G). Taken together, these results indicate that 6-G attenuates myocardial injury closely linked to its critical role in regulating autophagy and H19.

6-G attenuates myocardial injury by relying on enhanced autophagy

To further explore the mechanism underlying the 6-G attenuation of H/R-induced cardiomyocyte injury, we treated HL-1 cells with H/R, H/R + 6-G and H/R + 6-G + 3-MA, of which 3-MA is a broadly used autophagy inhibitor. The results showed that H/R inhibited cellular LC3 expression, whereas 6-G reversed the inhibitory effect of H/R on LC3 protein levels. Furthermore, the introduction of 3-MA remarkably blocked the increase in LC3 protein levels caused by the addition of 6-G (Fig. 2A). We also detected the expression of two autophagy-related factors, Beclin-1 and P62. The results indicated that 6-G was able to reverse the H/R-induced decrease in Beclin-1 as well as the increase in P62 (Fig. 2B). Simultaneously, cell

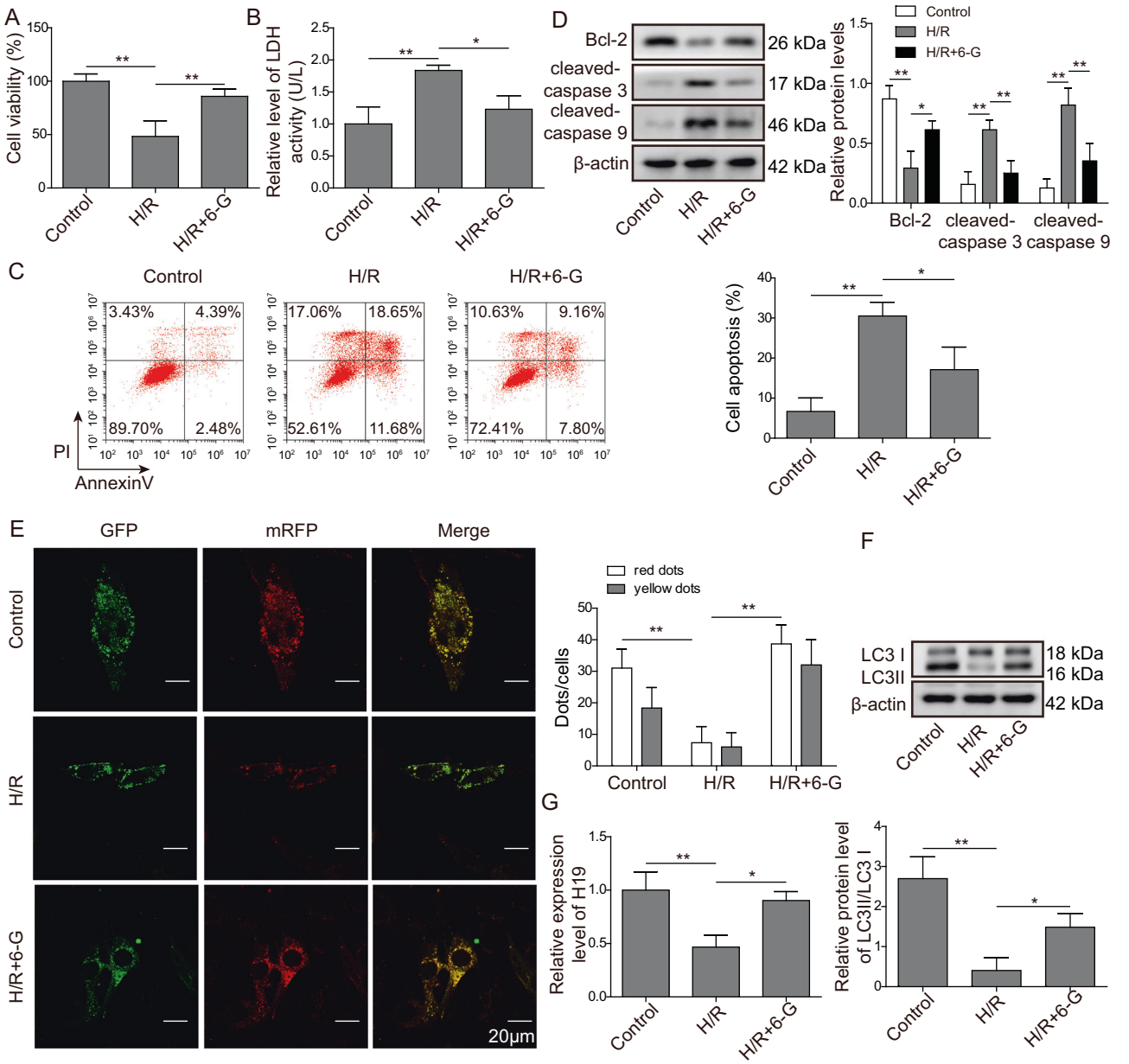

Fig. 1 6-G attenuates H/R-induced cardiomyocyte injury and enhances autophagy. Cell viability was determined by CCK-8 assay (**A**). Cytotoxic activity was determined by LDH kits (**B**). Cell apoptosis was detected by flow cytometry (**C**). The protein levels of Bcl-2, cleaved caspase 3, and caspase 9 were detected by western blot (**D**). Autophagic flux was analysed by transfection with mRFP-GFP-LC3 adenovirus (**E**). The expression of LC3 was evaluated by western blot (**F**). The relative expression level of H19 was determined using qPCR (**G**). $*P < 0.05$; $**P < 0.01$.

viability, membrane damage, and apoptosis were assessed in HL-1 cells treated with H/R or its combination with 6-G or 6-G plus 3-MA. Cell viability was decreased in H/R cells compared with the control, which was further elevated by adding 6-G alone rather than 6-G plus 3-MA. Similarly, 6-G severely restricted H/R-induced cell apoptosis and cytotoxicity only in the absence of 3-MA (Fig. 2C–E). In line with these results, H/R challenge impaired the amount of Bcl-2 but promoted the amount of cellular cleaved caspase 3 and caspase 9, whose expression was reversed in the 6-G group but not in the 6-G plus 3-MA group (Fig. 2F). Alternatively, using chloroquine as an autophagy inhibitor, we obtained similar results to those of 3-MA treatment regarding the effect of 6-G on autophagy pathways (Fig. S1). The above results strongly suggest that the alleviation of H/R-induced myocardial injury by 6-G most likely relies on its role in promoting the cellular autophagy process.

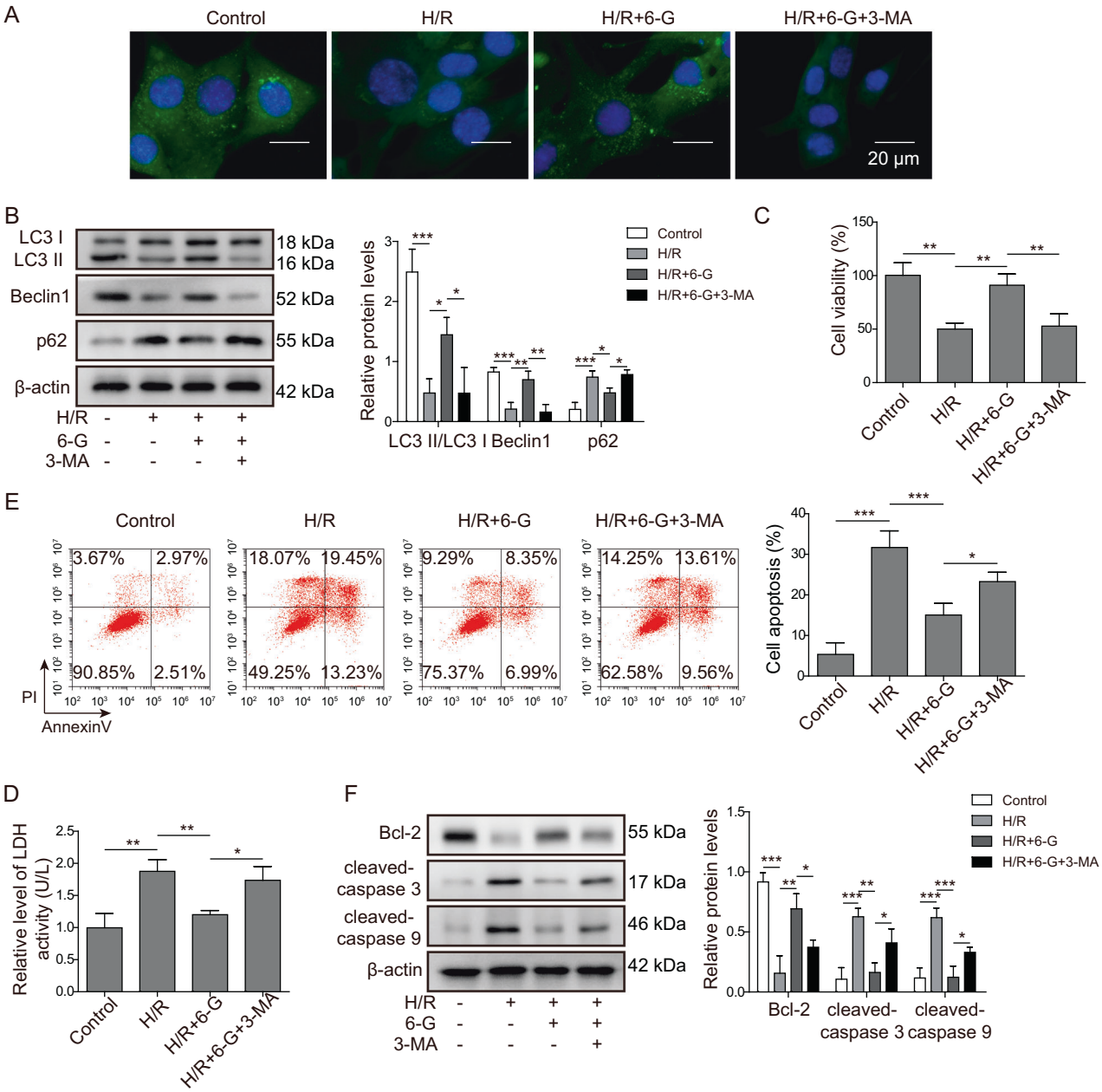

Fig. 2 6-G attenuates myocardial injury by relying on enhanced autophagy. HL-1 cells were treated with 6-G or its combination with 3-MA after challenge with H/R. Subsequently, the expression of LC3 was assessed by immunofluorescence (**A**). The expression of Beclin-1, LC3, and p62 were detected by western blot (**B**). Cell viability was determined by CCK-8 assay (**C**). Cytotoxic activity was determined by LDH kits (**D**). Cell apoptosis was detected by flow cytometry (**E**). The protein levels of Bcl-2, cleaved caspase 3, and caspase 9 were determined by western blot. $*P < 0.05$; $**P < 0.01$; $***P < 0.001$.

6-G promotes autophagy by upregulating H19 and relieves cardiomyocyte injury caused by H/R

In Fig. 1G, we showed that H19 was downregulated by H/R challenge and upregulated by treatment with 6-G, which prompted us to test its role in MIRI. First, as shown in Fig. 3A, H19 shRNA constructs were used to knockdown its expression in HL-1 cells. We next transfected sh NC or sh H19 into 6-G pretreated H/R challenged HL-1 cells and tested its effect on the autophagy process. In mRFP-GFP-LC3B-transfected cells, we observed that 6-G treatment significantly increased yellow and red puncta, which were further reduced by knockdown of H19 (Fig. 3B). Moreover, we demonstrated that LC3II and Beclin-1 expression was increased, whereas p62 expression was decreased in 6-G- or 6-G plus sh NC-treated cells. However, knockdown of H19 indeed reversed the effect of 6-G on the expression of these autophagic proteins (Fig. 3C). In

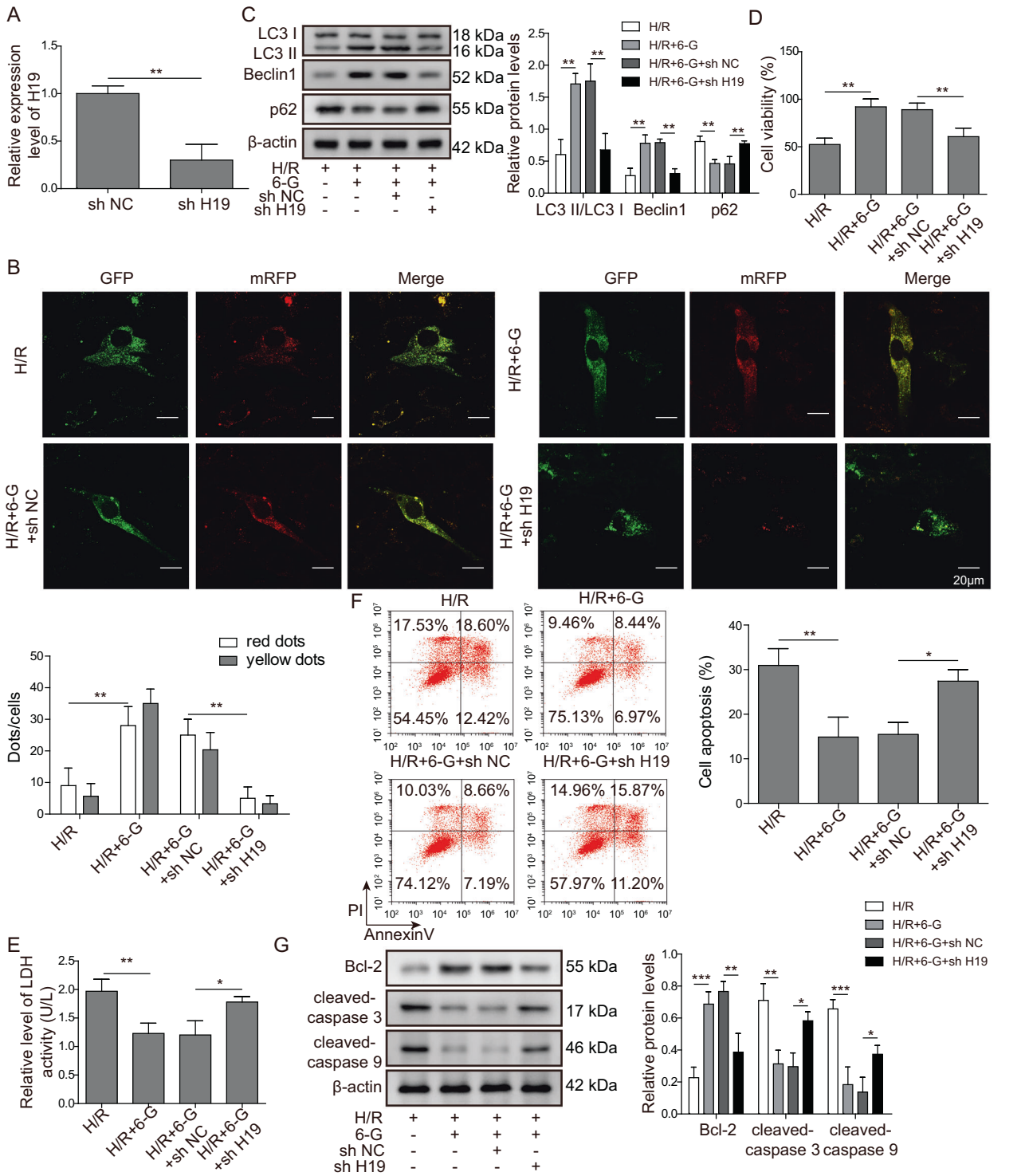

Fig. 3 6-G promotes autophagy by upregulating H19 and relieves cardiomyocyte injury caused by H/R. Knockdown efficiency of sh H19 was determined by qPCR (**A**). H/R-challenged HL-1 cells were treated with 6-G and further transfected with sh NC or sh H19, and autophagic flux was analysed by transfection with mRFP-GFP-LC3 adenovirus (**B**). The expression of Beclin-1, LC3, and p62 was detected by western blot (**C**). Cell viability was determined by CCK-8 assay (**D**). Cytotoxic activity was determined by LDH kits (**E**). Cell apoptosis was detected by flow cytometry (**F**). The protein levels of Bcl-2, cleaved caspase 3, and caspase 9 were determined by western blot (**G**). $^{*}P < 0.05$; $^{**}P < 0.01$; $^{***}P < 0.001$.

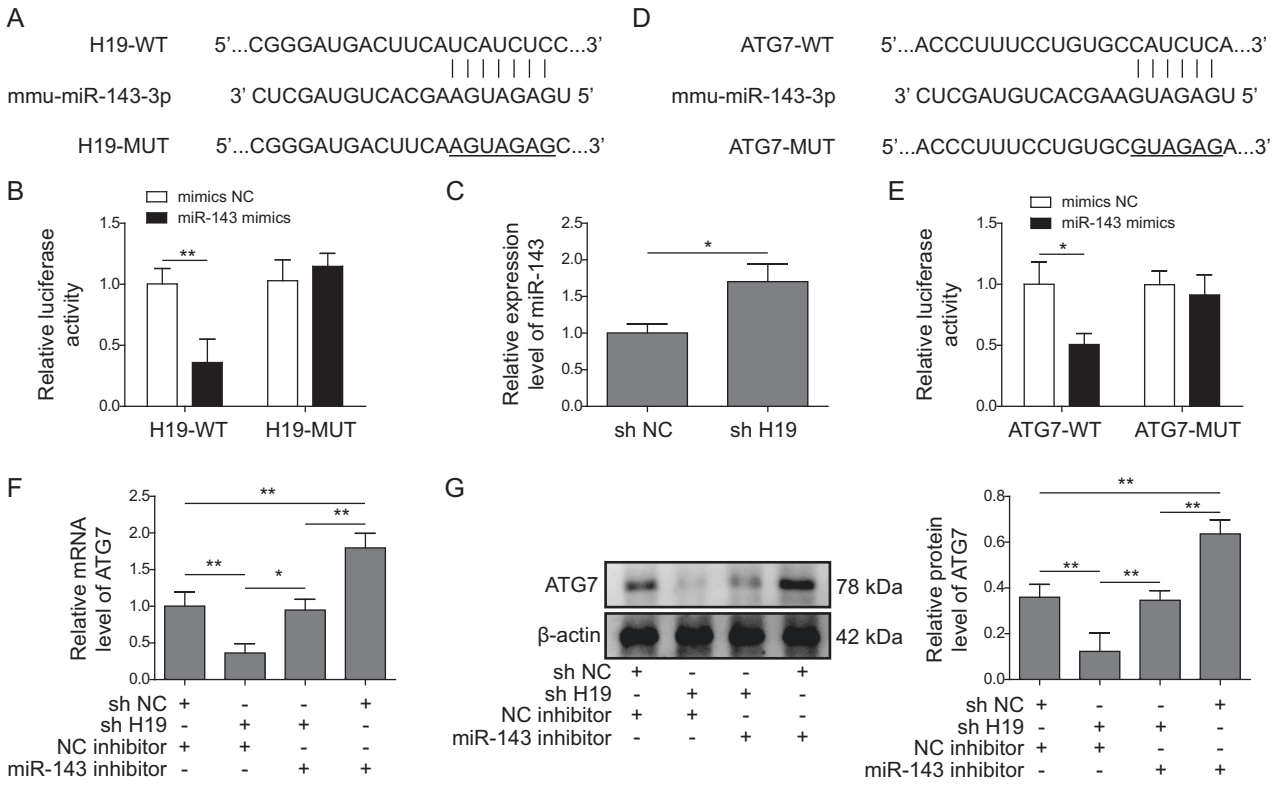

Fig. 4 H19 acts as a ceRNA by absorbing miR-143 and indirectly upregulates ATG7 expression. The binding sequence between miR-143-3p and H19 was predicted by StarBase software (**A**). miR-143 mimics or mimics NC were cotransfected with a luciferase reporter vector containing wild-type H19 or its mutant version. The interplay between miR-143 and H19 was validated by a dual-luciferase reporter assay (**B**). Relative expression of miR-143 was measured by qPCR in sh NC- or sh H19-transfected HL-1 cells (**C**). The binding sequence between miR-143-3p and ATG7 was predicted by StarBase software (**D**). Relative luciferase activity was measured by a dual-luciferase reporter assay in cells cotransfected with miR-143 and ATG7 3′-UTR or its mutant constructs (**E**). Relative mRNA and protein levels of ATG7 were detected by qPCR (**F**) and western blot (**G**), respectively. $^{*}P < 0.05$; $^{**}P < 0.01$.

addition, in H/R-treated HL-1 cells, 6-G profoundly lost its ability to increase cell viability when cellular H19 was knocked down (Fig. 3D). On the other hand, however, the inhibitory effect of 6-G on cytotoxicity and apoptosis was largely weakened when cells were transfected with sh H19 (Fig. 3E, F). In agreement, we observed that lower H19 expression gave rise to attenuated regulation of Bcl-2, cleaved caspase 3, and caspase 9 caused by 6-G (Fig. 3G). These results demonstrate that 6-G-promoted upregulation of H19 triggered the cellular autophagy process, thereby attenuating H/R-induced cardiomyocyte injury.

H19 acts as a ceRNA by absorbing miR-143 and indirectly upregulates ATG7 expression

To further investigate the regulatory mechanisms of H19 in MIRI, bioinformatics analysis was used to predict target genes. As shown in Fig. 4A, the binding site of miR-143-3p in the H19 sequence was obtained by using the StarBase online database (http://starbase.sysu.edu.cn/). The subsequent luciferase activity assay demonstrated that the luciferase activity was notably decreased in cells cotransfected with miR-143 and wild-type H19 compared to that of the mutant H19 vector (Fig. 4B). Moreover, miR-143 was upregulated in sh H19-transfected HL-1 cells compared to those cells transfected with sh NC (Fig. 4C). Similarly, ATG7, which codes for an enzyme essential for autophagy, was shown to be targeted by miR-143 (Fig. 4D). In the dual-luciferase reporter assay, the luciferase activity of HL-1 cells driven by ATG7-WT was found to be repressed by miR-143-3p but not by mimics NC (Fig. 4E). Furthermore, depletion of H19 caused a significantly decreased expression of ATG7, whereas miR-143 inhibitor resulted in enhanced ATG7 expression in terms of both mRNA and protein. However, the miR-143 inhibitor partially rescued the H19-induced reduction in ATG7 expression (Fig. 4F, G). Collectively, these data suggest that H19 most likely acts as a ceRNA by absorbing cellular miR-143, thereby regulating ATG7 expression.

The H19/miR-143/ATG7 axis is required for 6-G to alleviate H/R injury

To further demonstrate the correlation of 6-G with autophagy signaling and the potential regulatory network of MIRI, we overexpressed ATG7 in HL-1 cells together with transfection of sh H19 and/or miR-143 inhibitors. Both ATG7 mRNA and protein were significantly increased in cells transfected with ATG7 compared with pcDNA3.1-transfected cells, indicating that ATG7 was successfully overexpressed in cells (Fig. 5A). Upon 6-G pretreatment, cellular LC3II and Beclin-1 levels were elevated, largely accompanied by downregulated P62. However, the protein levels of LC3II, Beclin-1, and P62 were reversed by knockdown of H19. Strikingly, the combination of sh H19 and miR-143 inhibitor or ATG7 again increased LC3II and Beclin-1 yet decreased P62 expression (Fig. 5B). Moreover, 6-G-pretreated cells exhibited higher cell activity but lower cytotoxicity and apoptosis than H/R-treated cells alone, which were further oppositely regulated by knockdown of H19. Importantly, we found that cotransfection of miR-143 inhibitor or ATG7 with sh H19 reversed the effect of H19 depletion on cell viability, cytotoxicity, and apoptosis (Fig. 5C–E). Next, we determined that 6-G promoted Bcl-2 and inhibited cleaved caspase 3 and cleaved caspase 9 expression induced by H/R. However, the introduction of sh H19 to these cells caused decreased Bcl-2 and enhanced cleaved caspase 3 and cleaved caspase 9 expression. In addition, combined transfection of miR-143 inhibitor or ATG7 with sh H19 produced an apparent positive effect on Bcl-2, but a negative effect on cleaved caspase 3 and cleaved caspase 9 levels (Fig. 5F). These results show that 6-G alleviates H/R-induced cardiomyocyte injury by promoting autophagy and inhibiting apoptosis, which is attributed to its regulatory role in the H19/miR-143/ATG7 signaling axis.

6-G relieves myocardial ischemia-reperfusion injury through promotion of autophagy in mice

To better understand the role of 6-G in I/R-induced cardiac injury, experiments in a mouse model were conducted. The data showed that LC3II was suppressed in the I/R-treated group compared with the sham-operated group, which was further promoted by 6-G administration. Nevertheless, inhibition of the autophagy process using 3-MA profoundly blocked the function of 6-G, which caused significant downregulation of LC3II, and Beclin-1, whereas upregulation of p62 (Fig. 6A, B). Moreover, I/R-treated mice showed an increased myocardial infarction area compared with sham-operated mice. 6-G treatment generated a notable reduction in infarct size, which was augmented by inhibiting the autophagy process (Fig. 6C). In parallel, we used the TUNEL assay to detect cardiomyocyte apoptosis. The results demonstrated that the apoptosis rate increased significantly in I/R-treated mice compared with sham-operated mice. The apoptosis rate was significantly reduced upon 6-G treatment, which was significantly reversed by 3-MA-mediated autophagy inhibition (Fig. 6D). In the western blotting assay, relative to the sham-operated group, I/R-treated mice maintained a lower level of Bcl-2 but a higher level of cleaved caspase 3 and cleaved caspase 9. In addition, 6-G treatment caused the opposite effect on these proteins, which were functionally antagonized by 3-MA treatment (Fig. 6E). Together, these results suggest that 6-G relieves MIRI by enhancing autophagy in vivo.

Discussion

MIRI is the leading cause of heart failure or cardiac death in patients with AMI [1, 19]. It is believed that inhibiting I/R-induced apoptosis has significant benefits for MIRI alleviation. In this study, we assessed the effect of 6-G on H/R-treated HL-1 cells and found that 6-G improved cell viability and reduced cytotoxicity as well as apoptosis. Intriguingly, we also observed increased expression of H19 together with the autophagic marker LC3II in 6-G-pretreated cells. However, the underlying mechanism for the action of 6-G in regulating H19 and autophagy pathways during MIRI progression is still worthy of further investigation.

In recent years, increasing evidence has indicated that the autophagy pathway is frequently regulated in response to MIRI [20, 21]. For instance, HSP70 suppresses cardiomyocyte necroptosis by inhibiting autophagy in MIRI [22]. Moreover, Fan et al. reported that rapamycin-induced activation of the autophagy pathway protects cells from H/R injury [23]. In this study, we revealed that blocking autophagy with 3-MA greatly restricted the ability of 6-G to increase cell viability and decrease apoptosis and cytotoxicity. In addition, the upregulation of LC3II and Beclin-1 by 6-G was also greatly inhibited by delivering 3-MA to cells. In accordance with our previous findings, pretreatment with 6-G could largely inhibit myocardial apoptosis induced by I/R [17], which, however, was reversed by additionally treating with 3-MA. Next, we used shRNA to knockdown the expression of H19 and further evaluated the potential effect on 6-G function. Surprisingly, in H/R-challenged HL-1 cells, depletion of H19 gave rise to a similar result as that of 3-MA-treated cells. Collectively, these results implied that the alleviation of H/R-induced myocardial injury by 6-G relied, to some extent, on the cellular autophagy process.

The implication of lncRNAs in MIRI has been extensively studied in recent years [10, 24]. In particular,

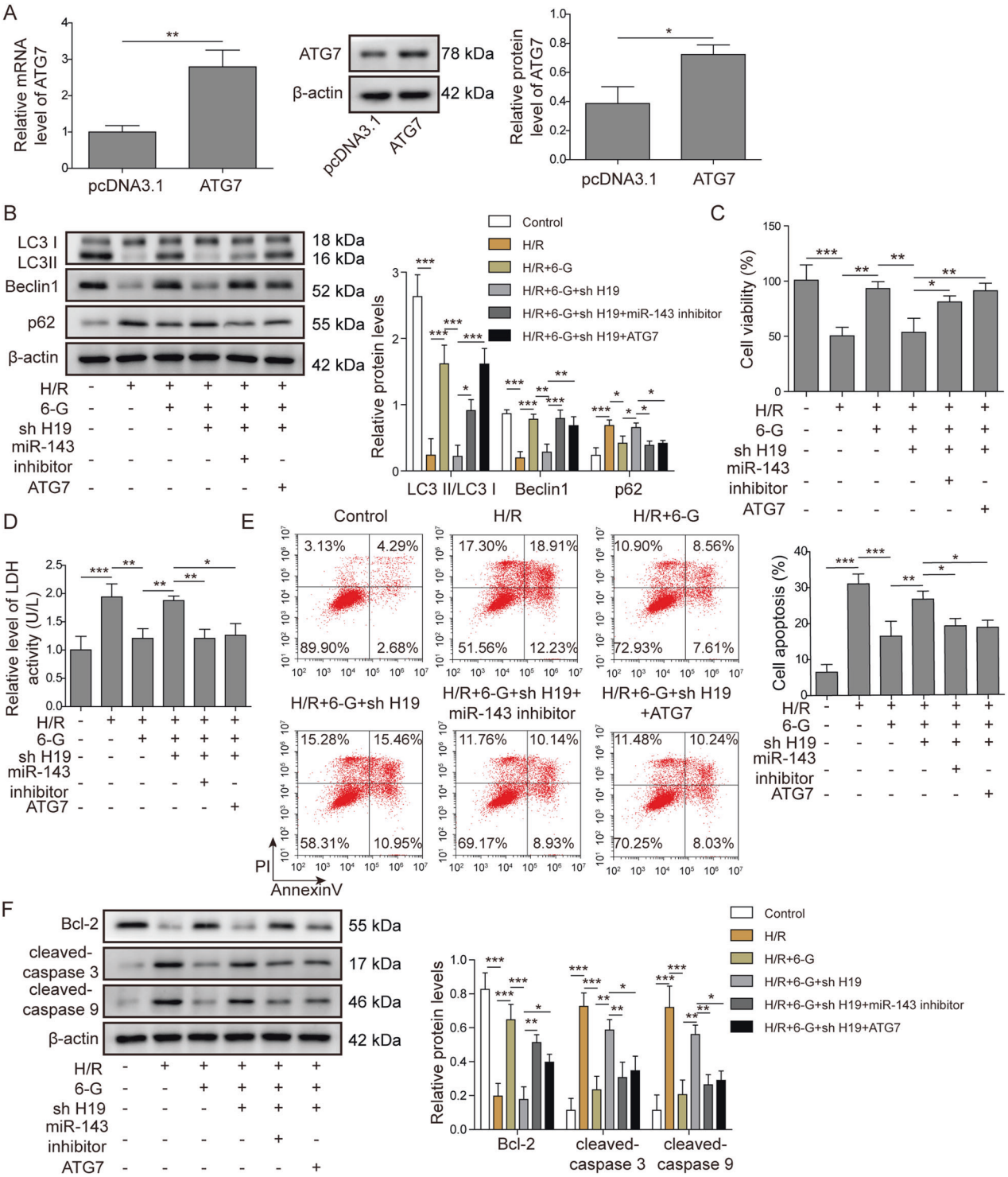

Fig. 5 The H19/miR-143/ATG7 axis is required for 6-G to alleviate H/R injury. Overexpression of ATG7 was verified using qPCR and western blot (**A**). H/R-challenged HL-1 cells were treated with 6-G and further transfected with sh H19, miR-143 inhibitor, or pCDNA-ATG7, and the protein levels of Beclin-1, LC3, and P62 in these cells were detected by western blot (**B**). Additionally, cell viability was determined by CCK-8 assay (**C**). Cytotoxic activity was determined by LDH kits (**D**). Cell apoptosis was detected by flow cytometry (**E**). The protein levels of Bcl-2, cleaved caspase 3, and caspase 9 were determined by western blot (**F**). $^{*}P < 0.05$; $^{**}P < 0.01$; $^{***}P < 0.001$.

lncRNAs play an essential role in diminishing cellular miRNAs by acting as competitive endogenous RNAs (ceRNAs), which thus relieve the inhibitory effect of miRNAs on their target genes. In MIRI, for example, lncRNA AK139328 reduces MIRI by inhibiting autophagy mediated by miR-204-3p [11]. Several reports have

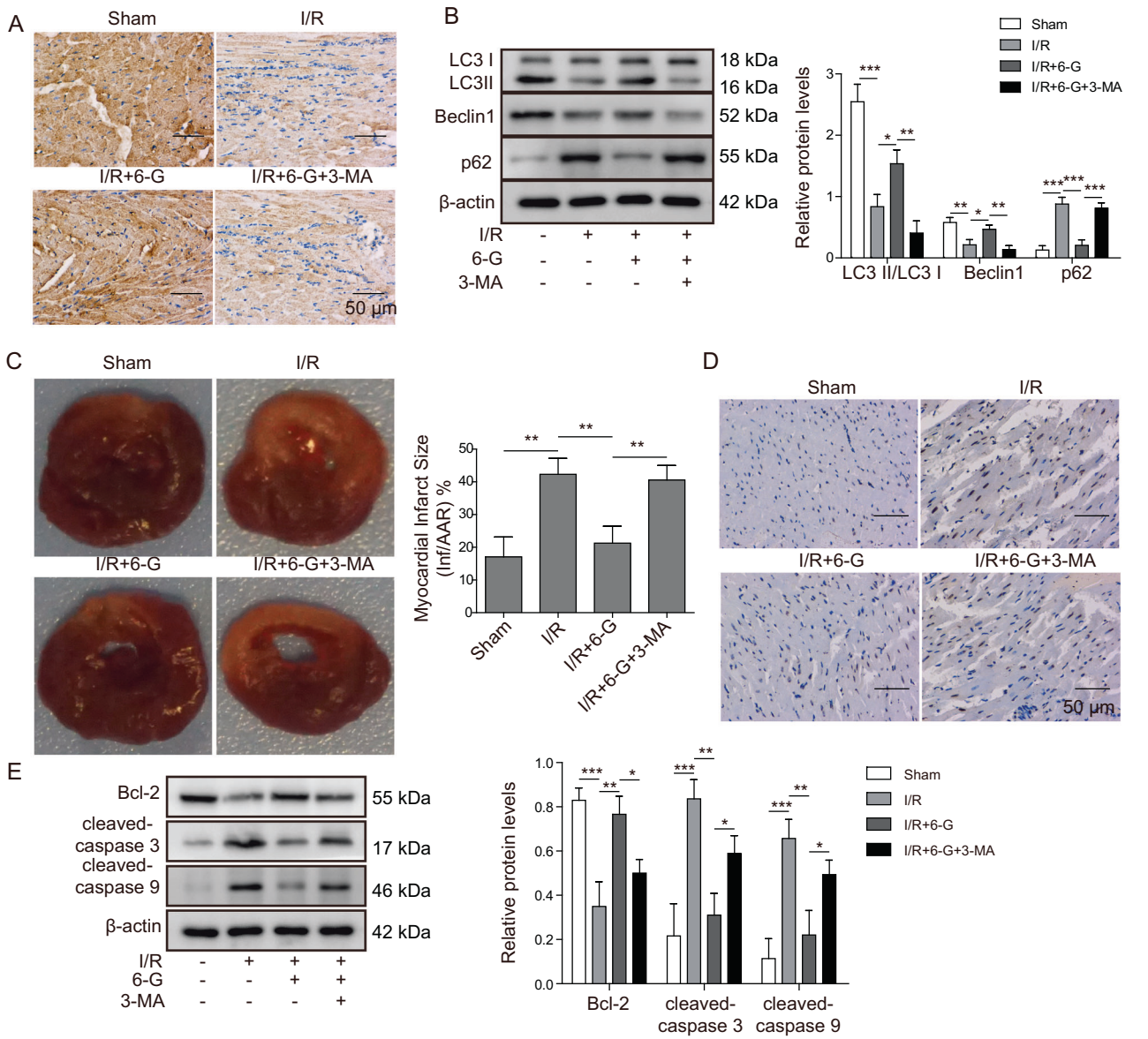

Fig. 6 6-G relieves myocardial ischemia-reperfusion injury through promotion of autophagy in mice. Expression levels of LC3 in mouse cardiac tissues were assessed with immunohistochemistry (**A**). Abundance of LC3, Beclin-1, and p62 protein was detected by western blot (**B**). The myocardial infarct area was evaluated by TTC staining (**C**). Cardiomyocyte apoptosis was examined by TUNEL assay (**D**). Protein levels of Bcl-2 and cleaved caspases 3 and 9 were measured by western blotting (**E**). $^{*}P < 0.05$; $^{**}P < 0.01$; $^{***}P < 0.001$.

documented the roles of H19 in regulating different miRNA families, including miR-139 [25], miR-455 [26], miR-877-3p [14], and their target genes, which further influence MIRI development. Our study demonstrated that miR-143 levels were significantly upregulated by depletion of cellular H19. The luciferase reporter assay confirmed the binding site of miR-143 in the H19 RNA transcript. In addition, we uncovered that H19 could enhance ATG7 expression by absorbing miR-143 from the ATG7 3′UTR, thereby promoting the autophagy process. Moreover, rescue experiments have shown that 6-G alleviates H/R-induced cardiomyocyte injury by regulating the H19/miR-143/ATG7 signaling axis. These results imply that the H19-miR-143-ATG7 regulatory pattern plays a critical role in MIRI development and is prone to be modulated by introducing 6-G.

To investigate the role of 6-G in the autophagy-mediated protective effect on H/R in a mouse model, 6-G or 6-G combinations with the autophagy inhibitor 3-MA were administered. The data indicated that 6-G increased the autophagic response in mice. More importantly, 6-G treatment generated a notable reduction in infarct size, which, however, was reversed by 3-MA, indicating that autophagy is indispensable for 6-G to protect mice from MIRI. On the other hand, in line with the results obtained from HL-1 cells, 6-G could reduce the occurrence of apoptosis in mice

by increasing Bcl-2 but decreasing cleaved caspase 3 and cleaved caspase 9 levels. Our previous findings suggested that 6-G pretreatment could alleviate I/R-induced myocardial injury by attenuating cellular PI3K/Akt-dependent inflammation [27]. It is possible that treatment with 6-G could lead to a reasonable level of autophagy and anti-inflammatory effects having a synergistic effect on alleviating MIRI.

In conclusion, our results demonstrate that 6-G pretreatment alleviates I/R-induced myocardial injury both in vitro and in vivo via upregulation of H19 expression, in turn promoting the cellular autophagy pathway by absorbing miR-143 from ATG7 3′UTR. Together, these data suggest that treatment with 6-G may be a promising method for the treatment of MIRI.

Data availability

All data generated or analyzed during this study are included in this article. The datasets used and/or analyzed during the current study are available from the corresponding author on reasonable request.

Acknowledgements We would like to give our sincere gratitude to the reviewers for their constructive comments.

Author contributions Conception and study design: Xiang-Wei Lv; Data acquisition: Meng-Jie Wang; Data analysis: Qiu-Yu Qin; Manuscript drafting: Pan Lu; Manuscript revising: Guo-Wei Qin.

Compliance with ethical standards

Ethical approval The animal ethics involved in the experiment was approved by the Guilin Medical University Laboratory Animal Ethics Committee.

Funding This study was supported by grants from the Natural Science Foundation of Guangxi (no. 2018GXNSFDA281039) and Natural Science Foundation of Guangxi (no.2018GXNSFAA294096).

Consent for publication The informed consent obtained from study participants.

Conflict of interest The authors declare no competing interests.

References

1. Writing Group M, Mozaffarian D, Benjamin EJ, Go AS, Arnett DK, Blaha MJ, et al. Heart disease and stroke statistics-2016 update: a report from the American Heart Association. Circulation. 2016;133:e38–360.
2. Gerczuk PZ, Kloner RA. An update on cardioprotection: a review of the latest adjunctive therapies to limit myocardial infarction size in clinical trials. J Am Coll Cardiol. 2012;59:969–78.
3. Hausenloy DJ, Yellon DM. Myocardial ischemia-reperfusion injury: a neglected therapeutic target. J Clin Invest. 2013;123:92–100.
4. Keeley EC, Boura JA, Grines CL. Primary angioplasty versus intravenous thrombolytic therapy for acute myocardial infarction: a quantitative review of 23 randomised trials. Lancet. 2003;361:13–20.
5. Neri M, Riezzo I, Pascale N, Pomara C, Turillazzi E. Ischemia/reperfusion injury following acute myocardial infarction: a critical issue for clinicians and forensic pathologists. Mediat Inflamm. 2017;2017:7018393.
6. Ye G, Fu Q, Jiang L, Li Z. Vascular smooth muscle cells activate PI3K/Akt pathway to attenuate myocardial ischemia/reperfusion-induced apoptosis and autophagy by secreting bFGF. Biomed Pharmacother. 2018;107:1779–85.
7. Zhang T, Ma Y, Gao L, Mao C, Zeng H, Wang X, et al. MicroRNA-146a protects against myocardial ischaemia reperfusion injury by targeting Med1. Cell Mol Biol Lett. 2019;24:62.
8. Mizushima N, Yoshimori T, Levine B. Methods in mammalian autophagy research. Cell. 2010;140:313–26.
9. Zhang HR, Bai H, Yang E, Zhong ZH, Chen WY, Xiao Y, et al. Effect of moxibustion preconditioning on autophagy-related proteins in rats with myocardial ischemia reperfusion injury. Ann Transl Med. 2019;7:559.
10. Li X, Dai Y, Yan S, Shi Y, Han B, Li J, et al. Down-regulation of lncRNA KCNQ1OT1 protects against myocardial ischemia/reperfusion injury following acute myocardial infarction. Biochem Biophys Res Commun. 2017;491:1026–33.
11. Yu SY, Dong B, Fang ZF, Hu XQ, Tang L, Zhou SH. Knockdown of lncRNA AK139328 alleviates myocardial ischaemia/reperfusion injury in diabetic mice via modulating miR-204-3p and inhibiting autophagy. J Cell Mol Med. 2018;22:4886–98.
12. Keniry A, Oxley D, Monnier P, Kyba M, Dandolo L, Smits G, et al. The H19 lincRNA is a developmental reservoir of miR-675 that suppresses growth and Igf1r. Nat Cell Biol. 2012;14:659–65.
13. Necsulea A, Soumillon M, Warnefors M, Liechti A, Daish T, Zeller U, et al. The evolution of lncRNA repertoires and expression patterns in tetrapods. Nature. 2014;505:635–40.
14. Li X, Luo S, Zhang J, Yuan Y, Jiang W, Zhu H, et al. lncRNA H19 alleviated myocardial I/RI via suppressing miR-877-3p/Bcl-2-mediated mitochondrial apoptosis. Mol Ther Nucleic Acids. 2019;17:297–309.
15. Luo H, Wang J, Liu D, Zang S, Ma N, Zhao L, et al. The lncRNA H19/miR-675 axis regulates myocardial ischemic and reperfusion injury by targeting PPARalpha. Mol Immunol. 2019;105:46–54.
16. Zhou M, Zou YG, Xue YZ, Wang XH, Gao H, Dong HW, et al. Long non-coding RNA H19 protects acute myocardial infarction through activating autophagy in mice. Eur Rev Med Pharmacol Sci. 2018;22:5647–51.
17. Lv X, Xu T, Wu Q, Zhou Y, Huang G, Xu Y, et al. 6-Gingerol activates PI3K/Akt and inhibits apoptosis to attenuate myocardial ischemia/reperfusion injury. Evid Based Complement Alternat Med. 2018;2018:9024034.
18. Wang S, Tian M, Yang R, Jing Y, Chen W, Wang J, et al. 6-Gingerol ameliorates behavioral changes and atherosclerotic lesions in ApoE(-/-) mice exposed to chronic mild stress. Cardiovasc Toxicol. 2018;18:420–30.
19. Sanchez-Hernandez CD, Torres-Alarcon LA, Gonzalez-Cortes A, Peon AN. Ischemia/reperfusion injury: pathophysiology, current clinical management, and potential preventive approaches. Mediat. Inflamm. 2020;2020:8405370.
20. Wang Y, Zhang K, Qi X, Yang G, Wang H, Zhang Z, et al. Effects of propofol on LC3II and mTOR/p-mTOR expression during ischemia-reperfusion myocardium injury in rats with type 2 diabetes mellitus. Exp Ther Med. 2020;19:2441–8.

21. Zhou LY, Zhai M, Huang Y, Xu S, An T, Wang YH, et al. The circular RNA ACR attenuates myocardial ischemia/reperfusion injury by suppressing autophagy via modulation of the Pink1/FAM65B pathway. Cell Death Differ. 2019;26:1299–315.
22. Liu X, Zhang C, Zhang C, Li J, Guo W, Yan D, et al. Heat shock protein 70 inhibits cardiomyocyte necroptosis through repressing autophagy in myocardial ischemia/reperfusion injury. In Vitro Cell Dev Biol Anim. 2016;52:690–8.
23. Fan T, Chen L, Huang Z, Wang W, Zhang B, Xu Y, et al. Autophagy activation by rapamycin before hypoxia-reoxygenation reduces endoplasmic reticulum stress in alveolar epithelial cells. Cell Physiol Biochem. 2017;41:79–90.
24. Han Y, Wu N, Xia F, Liu S, Jia D. Long noncoding RNA GAS5 regulates myocardial ischemiareperfusion injury through the PI3K/AKT apoptosis pathway by sponging miR5325p. Int J Mol Med. 2020;45:858–72.
25. Gong LC, Xu HM, Guo GL, Zhang T, Shi JW, Chang C. Long non-coding RNA H19 protects H9c2 cells against hypoxia-induced injury by targeting MicroRNA-139. Cell Physiol Biochem. 2017;44:857–69.
26. Huang ZW, Tian LH, Yang B, Guo RM. Long noncoding RNA H19 acts as a competing endogenous RNA to mediate CTGF expression by sponging miR-455 in cardiac fibrosis. DNA Cell Biol. 2017;36:759–66.
27. Xu T, Qin G, Jiang W, Zhao Y, Xu Y, Lv X. 6-Gingerol protects heart by suppressing myocardial ischemia/reperfusion induced inflammation via the PI3K/Akt-dependent mechanism in rats. Evid Based Complement Alternat Med. 2018;2018:6209679.